Available online at www.sciencedirect.com

SciVerse ScienceDirect

Ceramics International 38 (2012) 6035–6039

CERAMICS INTERNATIONAL

www.elsevier.com/locate/ceramint

Short communication

Mechanical synthesis and rapid consolidation of nanostructured FeAl–Al_2O_3 composites by high-frequency induction heated sintering

In-Jin Shon [a,*], Seung-Hoon Jo [a], Jung-Mann Doh [b], Jin-Kook Yoon [b], Bang-Ju Park [c]

[a] Division of Advanced Materials Engineering and Research Center for Advanced Materials Development, Engineering College, Chonbuk National University, 664-14 Deokjin-dong 1-ga, Deokjin-gu, Jeonju, Jeonbuk 561-756, Republic of Korea

[b] Advanced Functional Materials Research Center, Korea Institute of Science and Technology, PO Box 131, Cheongryang, Seoul 130-650, Republic of Korea

[c] College of BioNano Tech., Gachon University, 1342 SeongnamDaero, Soojung-gu, Seongnam-si, Gyeonggi-do 461-701, Republic of Korea

Received 7 July 2011; received in revised form 25 March 2012; accepted 29 March 2012

Available online 5 April 2012

Abstract

Nanopowders of FeAl and Al_2O_3 were synthesized from Fe_2O_3 and Al by high energy ball milling. The sizes of FeAl and Al_2O_3 were 4 and 57 nm, respectively. A dense nanostuctured FeAl–Al_2O_3 composite was consolidated by a high-frequency induction heated sintering method within two minutes from mechanically synthesized powders of FeAl and Al_2O_3. The grain size, sintering behavior and hardness of the sintered FeAl–Al_2O_3 composite were investigated.

Keywords: B. Composites; C. Hardness; Mechanical alloy; Nanomaterials; High-frequency induction heated sintering

1. Introduction

Iron aluminide (FeAl) is interesting for structural applications at elevated temperature in hostile environments. This is because it generally possesses excellent oxidation and corrosion resistance, relatively lower density and lower material cost than Ni-based alloys [1,2]. However, its use has been limited by its brittleness at room temperature. To improve on the mechanical properties of these materials, the fabrication of nanostructured material and the addition of a second phase to form composites [3–5] have been found to be effective.

Conventional methods of processing iron aluminides, including casting, hot rolling and powder metallurgy, have been investigated [6,7]. However, none of these methods yield nanostructures. Recently, nanocrystalline powders have been produced by high energy milling [8]. The sintering temperature of high energy mechanically milled powder is lower than that of unmilled powder due to the increased reactivity, internal and surface energies, and surface area of the milled powder, which contribute to its so-called mechanical activation [9–11].

Nanocrystalline materials have received much attention as advanced engineering materials with improved physical and mechanical properties [12,13]. As nanomaterials possess a high strength, high hardness, excellent ductility and toughness, undoubtedly, more attention has been paid for their applications [14]. The grain size in sintered materials becomes much larger than that in pre-sintered powders due to rapid grain growth during a conventional sintering process. Therefore, controlling grain growth during sintering is one of the keys to the commercial success of nanostructured materials. In this regard, the high frequency induction heated sintering method (HFIHSM), which can make dense materials within 2 min, has been shown to be effective in achieving not only rapid densification to near theoretical density but also the hindrance of grain growth in nano-structured materials [15,16].

This paper reports on an investigation on mechanical synthesis of nanopowder of FeAl and Al_2O_3 and a dense nanocrystalline FeAl–Al_2O_3 composite within two minutes starting with high energy ball milled nanopowder using this high-frequency induction heated sintering method. The mechanical properties and grain sizes of the resulting nanostructured FeAl–Al_2O_3 composite are also evaluated.

* Corresponding author. Tel.: +82 63 270 2381; fax: +82 63 270 2386.
E-mail address: ijshon@chonbuk.ac.kr (I.-J. Shon).

0272-8842/$36.00
http://dx.doi.org/10.1016/j.ceramint.2012.03.073

2. Experimental procedures

Powders of 99% Fe_2O_3 (<5 nm, Alfa, Inc.) and 99% pure Al (−200 mesh, Samchun Pure Chemical Co., Inc.) were used as a starting materials. Fe_2O_3 and 4Al powders were mixed by a high-energy ball mill, Pulverisette-5 planetary mill at 250 rpm for 10 h. Tungsten carbide balls (8.5 mm in diameter) were used in a sealed cylindrical stainless steel vial under an argon atmosphere. The weight ratio of ball-to-powder was 30:1. The grain sizes of FeAl and Al_2O_3 were calculated by Suryanarayana and Grant Norton's formula [17]:

$$B_r(B_{crystalline} + B_{strain})\cos\theta = \frac{k\lambda}{L + \eta\sin\theta} \quad (1)$$

where B_r is the full width at half-maximum (FWHM) of the diffraction peak after instrumental correction; $B_{crystalline}$ and B_{strain} are the FWHM caused by the small grain size and internal strain, respectively; k is a constant (with a value of 0.9); λ is the wavelength of the X-ray radiation; L and η are grain size and internal strain, respectively; and θ the Bragg angle. The parameters B and B_r follow Cauchy's form with the relationship: $B = B_r + B_s$, where B and B_s are the FWHM of the broadened Bragg peaks and a standard sample's Bragg peaks, respectively. After milling, the mixed powders were placed in a graphite die (outside diameter, 45 mm; inside diameter, 20 mm; height, 40 mm) and then introduced into the high-frequency induction heated sintering system made by Eltek in South Korea shown in Fig. 1. The four major stages in the sintering are as follows. The system was evacuated (stage 1). And a uniaxial pressure of 80 MPa was applied (stage 2). An induced current was then activated and maintained until densification was attained as indicated by a linear gauge measuring the shrinkage of the sample (stage 3). Temperature was measured by a pyrometer focused on the surface of the graphite die. At the end of the process, the sample was cooled to room temperature (stage 4).

The relative densities of the synthesized sample were measured by the Archimedes method. Microstructural information was obtained from product samples which were polished and etched using a solution of H_2SO_4 (20 vol.%) and H_2O (80 vol.%) for 35 s at room temperature. Compositional and micro structural analyses of the products were made through X-ray diffraction (XRD) and scanning electron microscopy (SEM) with energy dispersive X-ray analysis (EDAX). Vickers hardness was measured by performing indentations at load of 20 kg and a dwell time of 15 s on the synthesized samples.

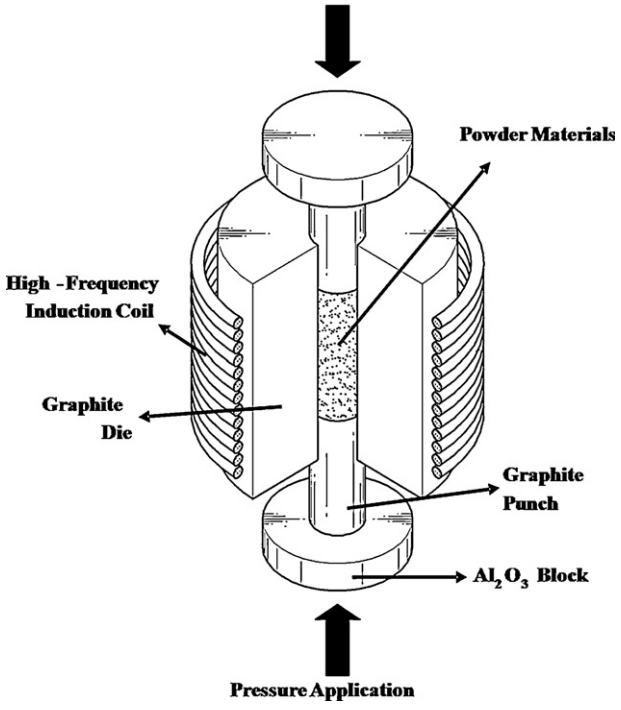

Fig. 1. Schematic diagram of apparatus for high-frequency induction heated sintering.

3. Results and discussion

XRD patterns of the milled powder are shown in Fig. 2. Reactant powders of Fe_2O_3 and Al peaks are not detected but product powders of FeAl and Al_2O_3 are detected. Therefore, it is considered that mechanical synthesis is produced during the high energy ball milling. Fig. 3 shows a FE-SEM image and X-ray mapping in the high energy ball milled powder of FeAl and Al_2O_3. In the FE-SEM image, the powders are very fine and agglomerated. Al and O are detected at the same point in the X-ray mapping. The average grain sizes of FeAl and Al_2O_3 calculated by Suryanarayana and Norton's formula were 4, and 40 nm, respectively.

The changes in shrinkage displacement and temperature of the surface of the graphite die with heating time during the processing of the FeAl and Al_2O_3 system are shown Fig. 4. As the induced current was applied, the shrinkage displacement of FeAl and Al_2O_3 continuously increased with temperature up to about 550 °C, and then abruptly increased. Fig. 5 shows XRD patterns of 2FeAl-Al_2O_3 composite sintered at 1250 °C. Only FeAl and Al_2O_3 peaks are detected. The structural parameters, i.e. the average grain sizes of FeAl and Al_2O_3 measured by

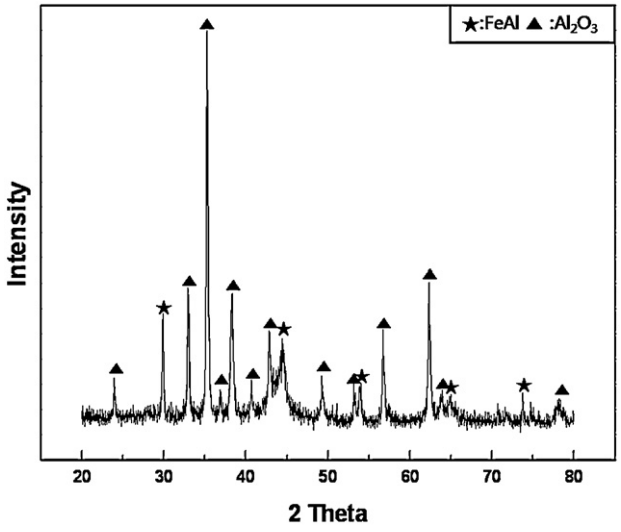

Fig. 2. XRD patterns of powder milled for 10 h.

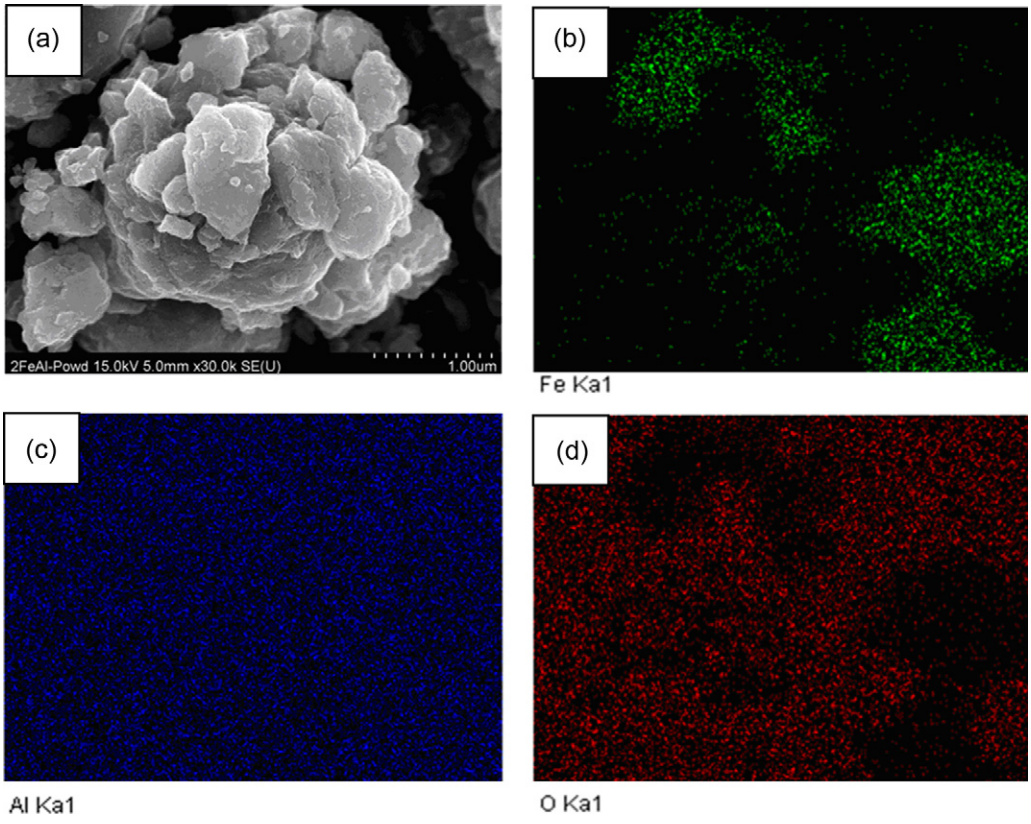

Fig. 3. Fe-SEM image (a) and X-ray mapping (b), (c) and (d) in high energy ball milled powders of Fe_2O_3–Al.

Suryanarayana and Norton's formula are 30 nm and 50 nm, respectively. And the relative density of 2FeAl–Al_2O_3 composite is about 95%. Fig. 6 shows FE-SEM image and EDS analysis for the FeAl–Al_2O_3 composite sintered from high energy ball milled powder. The composite consists of nanocrystalline material. In EDS, only Fe, Al and O were detected and heavier contaminations, such as WC from milling balls was not detected.

The role of the current (resistive or inductive) in sintering and or synthesis has been focus of several attempts aimed at providing an explanation to the observed enhancement of sintering and the improved characteristics of the products. The role played by the current has been variously interpreted, the effect being explained in terms of fast heating rate due to Joule heating, the presence of plasma in pores separating powder

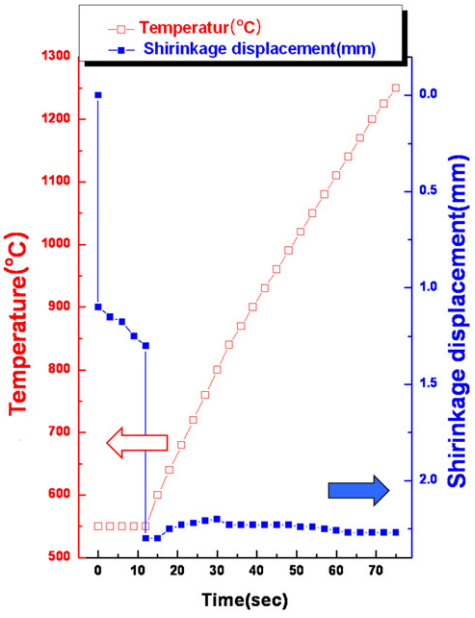

Fig. 4. Variations of the temperature and shrinkage displacement with heating time during high-frequency induction heated sintering of the FeAl–Al_2O_3 system.

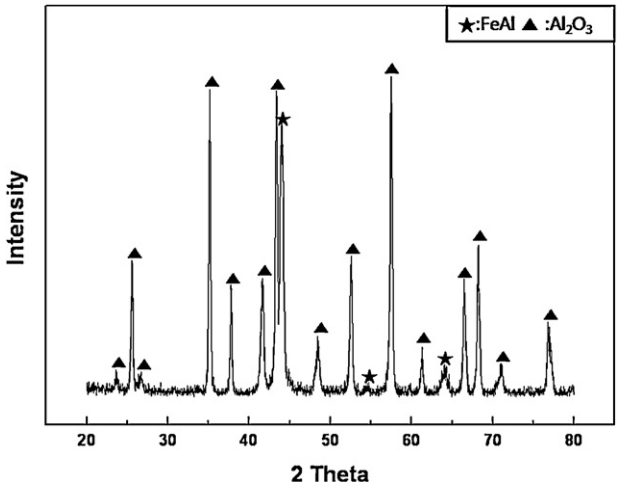

Fig. 5. XRD patterns of the FeAl–Al_2O_3 composite sintered at 1250 °C from high energy ball milled powder.

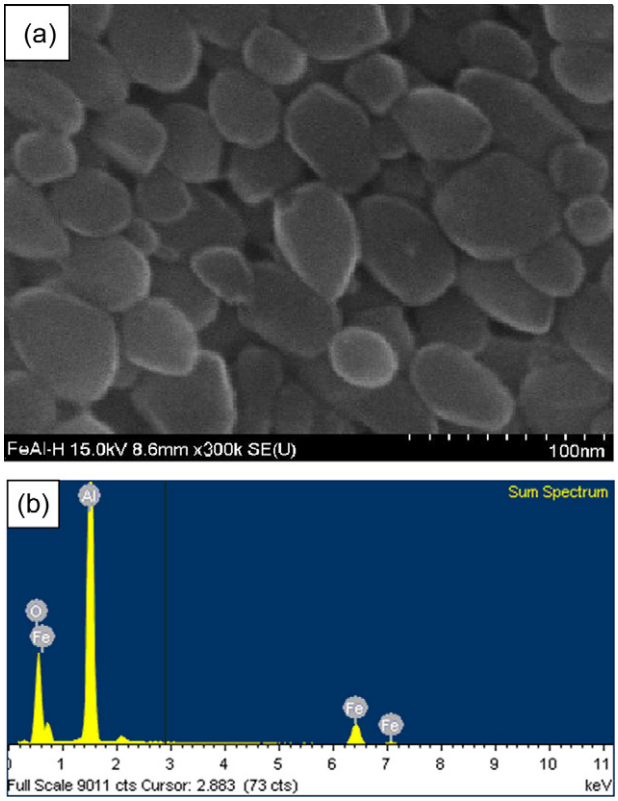

Fig. 6. FE-SEM image of the FeAl–Al_2O_3 composite sintered at 1250 °C.

particles, and the intrinsic contribution of the current to mass transport [18–21].

Vickers hardness measurements were made on polished sections of the 2FeAl–Al_2O_3 composite using a 20 kg_f load and 15 s dwell time. The calculated hardness values of the FeAl–Al_2O_3 composite sintered from high energy ball milled powder were 600 ± 15 kg/mm^2. This value represents an average of five measurements. Fig. 7 shows Vickers hardness indentation in FeAl–Al_2O_3 composite. Cracks were not observed to propagate from the indentation corners and fracture toughness cannot be calculated from crack length. Godlewska et al. investigated FeAl sintered from self-propagating high-temperature synthesized powders followed by hot forging. The hardness and grain sizes of their FeAl were 274 kg/mm^2 and 24 (radial) μm, 8.2 (axial) μm [22]. The hardness in this study is higher than that of Goglewska et al.'s study due to a refinement of the grain size and the addition of Al_2O_3.

4. Conclusions

Nanopowders of FeAl and Al_2O_3 were synthesized from Fe_2O_3 and Al during the high-energy ball milling for 10 h. Using the high-frequency induction heated sintering method, the densification of nanostructured 2FeAl–Al_2O_3 was accomplished from mechanically synthesized powder of FeAl–Al_2O_3. A nearly full density of 2FeAl–Al_2O_3 composites can be achieved within two minutes with an applied pressure of 80 MPa and the induced current. The average grain sizes of the FeAl and Al_2O_3 are 48 nm and 60 nm, respectively. And the

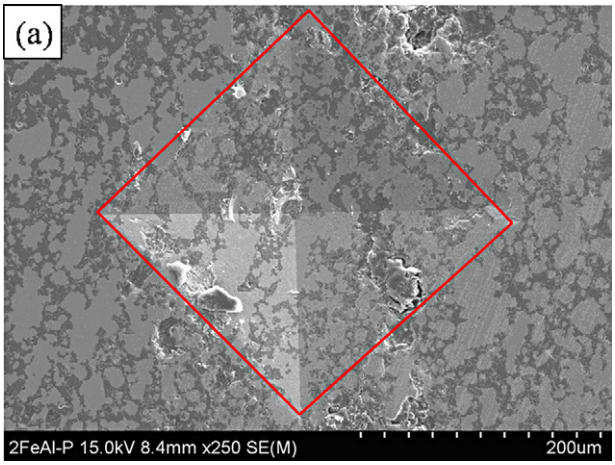

Fig. 7. Vickers hardness indentation in the FeAl–Al_2O_3 composite.

relative density of 2FeAl–Al_2O_3 composite is about 95%. The calculated hardness values of the FeAl–Al_2O_3 composite sintered from high energy ball milled powder were 600 ± 15 kg/mm^2.

Acknowledgments

This work is partially supported by KIST Future Resource Research Program and by the Human Resources Development of the Korea Institute of Energy Technology Evaluation and Planning (KETEP) grant funded by the Korea government Ministry of Knowledge Economy (No. 20114030200060).

References

[1] C.T. Liu, E.P. George, P.J. Maziasz, J.H. Schneibel, Recent advances in B2 iron aluminides alloys: fracture and alloy design, Materials Science and Engineering A 258 (1998) 84–98.
[2] S.C Deevi, V.K. Sikka, Nickel and iron aluminides: an overview on properties, processing, and application, Intermetallics 4 (1996) 357–375.
[3] Y. Ohya, M.J. Hoffmann, G. Petzow, Sintering of in situ synthesized SiC–TiB_2 composites with improved fracture toughness, Journal of the American Ceramic Society 75 (1992) 2479–2483.
[4] S.K. Bhaumik, C. Divakar, A.K. Singh, G.S. Upadhyaya, Synthesis and sintering of TiB_2 and TiB_2–TiC composite under high pressure, Materials Science and Engineering Part A 279 (2000) 275–281.
[5] D.Y. Oh, H.C. Kim, J.K. Yoon, I.J. Shon, One step synthesis of dens MoSi2–SiC composite by high-frequency induction heated combustion and its mechanical properties, Journal of Alloys and Compounds 395 (2005) 174–180.
[6] V.K. Sikka, in: Proceedings of the 5th Annual Conference on Fossil Energy Materials, Oak Ridge, TN, (1991), p. 197.
[7] J.R. Knibloe, R.N. Wright, V.K. Sikka, in: E.R. Andreotti, P.J. McGreehan (Eds.), Advances in Powder Metallurgy, Metal powder Industries Federation, Princeton, NJ, 1990, p. 219.
[8] D.M. Lee, K.M. Jo, I.J. Shon, Fabrication of 4.25$Co_{0.53}Fe_{0.47}$–Al_2O_3 composite by high frequency induction heated combustion synthesis and sintering, Journal of the Korean Institute of Metals and Materials 47 (2009) 344–348.
[9] F. Charlot, E. Gaffet, B. Zeghmati, F. Bernard, J.C. Liepce, Mechanically activated synthesis studied by X-ray diffraction in the Fe–Al system, Materials Science and Engineering A262 (1999) 279–288.
[10] V. Gauthier, C. Josse, F. Bernard, E. Gaffet, J.P. Larpin, Synthesis of niobium aluminides using mechanically activated self-propagating high-temperature

synthesis and mechanically activated annealing process, Materials Science and Engineering A265 (1999) 117–128.
[11] M.K. Beyer, H. Clausen-Schaumann, Mechanochemistry: the mechanical activation of covalent bonds, Chemical Reviews 105 (2005) 2921–2948.
[12] M.S. El-Eskandarany, Structure and properties of nanocrystalline TiC full-density bulk alloy consolidated from mechanical reacted powders, Journal of Alloys and Compounds 305 (2000) 225–238.
[13] L. Fu, L.H. Cao, Y.S Fan, Two-step synthesis of nanostructured tungsten carbide–cobalt powders, Scripta Materialia 44 (2001) 1061–1068.
[14] S. Berger, R. Porat, R. Rosen, Nanocrystalline materials: a study of WC-based hard metals, Progress in Materials Science 42 (1997) 311–320.
[15] D.Y. Oh, H.C. Kim, J.K. Yoon, I.J. Shon, Simultaneous synthesis and consolidation process of ultra-fine WSi_2–SiC and its mechanical propertes, Journal of Alloys and Compounds 386 (2005) 270–275.
[16] I.J. Shon, S.C. Kim, B.S. Lee, B.R. Kim, Pulsed current activated combustion synthesis and consolidation of nanostructured $ReSi_{1.75}$, Electronic Materials Letters 5 (2009) 19–22.
[17] C. Suryanarayana, M. Grant Norton, X-ray Diffraction A Practical Approach, Plenum Press, 1998,, p. 213.
[18] Z. Shen, M. Johnsson, Z. Zhao, M. Nygren, Spark plasma sintering of alumina, Journal of the American Ceramic Society 85 (2002) 1921–1927.
[19] J.E. Garay, U. Anselmi-Tamburini, Z.A. Munir, S.C. Glade, P. Asoka-Kumar, Electric current enhanced defect mobility in Ni_3Ti intermetallic electric current enhanced defect mobility in Ni_3Ti intermetallics, Applied Physics Letters 85 (2004) 573–575.
[20] J.R. Friedman, J.E. Garay, U. Anselmi-Tamburini, Z.A. Munir, Modified interfacial reactions in Ag–Zn multilayers under the influence of high DC currents, Intermetallics 12 (2004) 589–597.
[21] J.E. Garay, J.E. Garay, U. Anselmi-Tamburini, Z.A. Munir, Enhanced growth of intermetallic phases in the Ni–Ti system by current effects, Acta Materialia 51 (2003) 4487–4495.
[22] E. Godlewska, S. Szczepanik, R. Mania, J. Krawiarz, S. Kozinski, FeAl materials from intermetallic powder, Intermetallics 11 (2003) 307–312.